Variable winds on Venus mapped in three dimensions

Augustin Sanchez-Lavega, Ricardo Hueso, Giuseppe Piccioni, Pierre Drossart, J. Peralta, S. Perez-Hoyos, Colin F. Wilson, Fred W. Taylor, Kevin H. Baines, David Luz, et al.

Decadal variations in equatorial Pacific ecosystems and ferrocline/pycnocline decoupling

Keith B. Rodgers,[1] Olivier Aumont,[2,3] Christophe Menkes,[2] and Thomas Gorgues[4]

Received 28 December 2006; revised 4 September 2007; accepted 26 December 2007; published 31 May 2008.

[1] The equatorial Pacific Ocean is known for its large interannual to decadal variability in circulation. In particular, the changes that occurred in 1976/1977 have received considerable attention in the climate dynamics literature, and recently there has been much attention focused on changes that may have occurred there in 1997/1998. Unfortunately, because of data sparsity, the impact of these changes or shifts on ocean biogeochemistry and ecosystems remains largely unknown. Here a three-dimensional ocean circulation model (the ORCA2 configuration of OPA) which has a food web/biogeochemistry model (PISCES) embedded in it, and which has been forced with both NCEP-1 and ERA-40 reanalysis fluxes over multiple decades, is used as a tool to investigate decadal changes and their associated mechanisms. Our main finding with the model is that a decrease in the amplitude of the surface zonal wind stress in the tropical Pacific in the mid-to-late-1970s leads to a decrease in Fe and Chl concentrations in the upwelling regions of the eastern equatorial Pacific after 1976/1977. These changes find expression predominantly during the upwelling season (the seasonal maximum for Fe and Chl concentrations), when surface Fe and Chl concentrations tend to be significantly higher pre-1976/1977 than post-1976/1977. The changes in Chl concentrations need to be understood as modulations of the amplitude of the seasonal cycle, rather than as a "biological regime shift" (an abrupt transition from one mean state to another). In contrast to what is found for Fe and Chl, for NO_3 the decadal changes in surface concentrations in the upwelling region about 1976/1977 can be described as a shift in the mean state. It is shown that the response in surface Fe and Chl in the upwelling region about 1976/1977 is proportionally larger than the decadal changes in surface wind stress forcing, and it is also larger than the previously reported change in the strength of the meridional overturning strength of the subtropical cells (STCs). Importantly, this amplified response reflects a decoupling of the ferrocline and pycnocline within the equatorial Pacific. In this way, the presence of a time-invariant sediment source for Fe can substantially amplify the ecosystem response to decadal variability in ocean circulation.

Citation: Rodgers, K. B., O. Aumont, C. Menkes, and T. Gorgues (2008), Decadal variations in equatorial Pacific ecosystems and ferrocline/pycnocline decoupling, *Global Biogeochem. Cycles*, *22*, GB2019, doi:10.1029/2006GB002919.

1. Introduction

[2] There is widespread evidence of decadal variability in equatorial Pacific biogeochemistry, ecosystems, and fisheries [*Chavez et al.*, 2003; *Lehodey et al.*, 2003]. For ecosystems and fisheries these decadal changes tend to be synchronous over the Pacific basin [*Kawasaki*, 1983; *Lluch-Belda et al.*, 1989, 1992; *Schwartzlose et al.*, 1999]. These changes have been referred to as "biological regime shifts" in the coupled ocean/atmosphere system associated with the Pacific Decadal Oscillation (PDO) [*Mantua et al.*, 1997]. Within this framework, basin-scale decadal changes in the coupled ocean/atmosphere system find expression in low-frequency variability in the depth of the thermocline in the upwelling region of the eastern equatorial Pacific, impacting the local vertical (advective and diffusive) supply of nutrients to the euphotic zone. During decades when the mean state of the eastern equatorial Pacific is warm, the local thermocline is deep, and the supply of nutrients to the euphotic zone is reduced. Conversely, during decades when the mean state is cold, the thermocline shoals, and the supply of nutrients to the euphotic zone is enhanced. Implicit in this argument is the assumption that the background nutrient distribution on isopycnal surfaces is relatively stationary.

[1]Atmospheric and Ocean Sciences Program, Princeton University, Princeton, New Jersey, USA.
[2]LOCEAN, Paris, France.
[3]Centre IRD de Bretagne, Plouzané, France.
[4]JISAO-School of Oceanography, University of Washington, Seattle, Washington, USA.

0886-6236/08/2006GB002919

[3] Importantly, this framework of ''regime shifts'' for understanding decadal variability in both the physical climate system and biogeochemistry/ecosystems often rests on the assumption that there is a slowly evolving decadal mode of variability in the physical climate system which is independent of El Niño. As the first baroclinic mode oceanic Rossby and Kelvin waves which are known to play a key role in the evolution of El Niño and La Niña events propagate across the equatorial Pacific ocean in much less than a decade, mechanisms proposed for ''regime shifts'' evoke basin-scale ocean adjustment processes which connect the extratropical regions of the Pacific Ocean to the equatorial region [*Latif and Barnett*, 1994; *Gu and Philander*, 1997; *Kleeman et al.*, 1998]. The key assumption that underlies the majority of mechanisms that have been proposed is that decadal variability in the mean state is best understood as consisting of small perturbations about a stationary basic state.

[4] More recently, an alternative framework for interpreting decadal variability in the physical coupled ocean/atmosphere system has been articulated. According to this view, at least an important component of tropical Pacific decadal variability is in fact best understood as a rectified low-frequency expression of El Niño/Southern Oscillation (ENSO) variability [*Timmermann*, 2003; *Rodgers et al.*, 2004a; *Cibot et al.*, 2005]. In the study of *Rodgers et al.* [2004a] it was shown using output from a coupled ocean/atmosphere model that the structures in SST and thermocline depth characteristic of tropical Pacific decadal variability are due to an asymmetry between the anomaly patterns associated with the model's El Niño and La Niña states, with this asymmetry reflecting a nonlinearity in ENSO variability. During periods when ENSO variability is large, the asymmetries in SST and thermocline depth leave a change in the mean state as a residual. Within this framework, at least an important component of the tropical decadal variability needs to be understood in terms of changes in the high-frequency (i.e., seasonal and interannual timescale) variability.

[5] Here we use a state-of-the-art ocean circulation model to address the question of decadal variability in ecosystems in the upwelling region of the equatorial Pacific. The model used here has an ocean biogeoechemistry/food web model embedded in it, and the model has been forced with reanalysis fluxes at the sea surface. We shall be particularly interested in understanding the circulation controls which can impact the supply of Fe into the euphotic zone in the upwelling region, as Fe is thought to be the limiting nutrient for primary productivity in this region [*Martin et al.*, 1991, 1994; *Coale et al.*, 1996]. Measurements of the vertical distribution of Fe in the equatorial pycnocline reveal that the concentration of Fe is low near the surface, and that it increases abruptly near the base of the euphotic zone [*Mackey et al.*, 2002].

[6] For the mean state, it is known that the source waters for the equatorial undercurrent (EUC) lie largely in the extratropics, with approximately 2/3 of the EUC water coming from the Southern Hemisphere (see *Rodgers et al.* [2003, Figure 1] for a map of the source regions derived using Lagrangian trajectories). En route to ventilating the equatorial thermocline, a significant fraction of the extratropical source waters are thought to pass through the low-latitude western boundary currents (LLWBCs) of the equatorial Pacific [*Fine et al.*, 1994], namely the New Guinea coastal undercurrent to the south of the equator and the Mindanao current to the north. Thus in addition to the preformed Fe concentrations set in the extratropical source regions and remineralization within the thermocline, Fe concentrations in the EUC can also be strongly influenced by processes in the regions where the LLWBCs bring thermocline water into contact with the continental shelves. These processes include turbidity currents and fluxes from sediments.

[7] In terms of decadal variability of equatorial Pacific circulation fields, *McPhaden and Zhang* [2002] have used a variety of observations and data products to describe decadal changes in the subtropical cells (STCs) connecting the equatorial upwelling region to their extratropical source regions. They argue that the STC overturning during the 1960s (a time of relatively cool sea surface temperatures in the upwelling region) was approximately 25% larger than the STC overturning during the 1980s and early 1990s (a time of relatively warm SSTs in the upwelling region). *McPhaden and Zhang* [2002] suggest that decadal timescale variability in STC transport (i.e., basin-scale Pacific Ocean variability) may lead to perturbed fluxes of nutrients into the equatorial upwelling region, thereby perturbing equatorial ecosystems.

[8] Here we are interested in testing the hypothesis that decadal changes in tropical wind stress forcing drives a decoupling of the ferrocline and pycnocline, and that this makes a first-order contribution to decadal changes in equatorial ecosystems. More specifically, we intend to test the hypothesis that it is decadal variability in the trade winds (i.e., tropical wind stresses) that control decadal variations in equatorial ecosystems, and that this local tropical forcing is able to dominate extratropical forcing on this timescale. Through the use of reanalysis forcing fields that span several decades we focus on decadal variability and ignore processes that can act on longer timescales. In posing this question within the framework of forced ocean model experiments, we do not address whether low-frequency (i.e., decadal) variability in the trade winds is itself due to processes confined to the tropics, or whether it is due to larger-scale processes.

[9] There are an increasing number of studies whereby an ecosystem model which includes Fe limitation has been imbedded in a fully three-dimensional OGCM and forced with interannually varying surface fluxes [*Christian et al.*, 2002a, 2002b; *Wang et al.*, 2006; *Gorgues et al.*, 2005]. To date these modeling studies have tended to focus on seasonal to interannual variability, and the extent to which primary productivity can vary on the timescales characteristic of El Niño. Given that we are interested in weighing the relative merits of the ''regime shift'' and ''rectifier'' frameworks for understanding decadal variability in equatorial ecosystems, in our analysis of decadal variability we will want to include variations on seasonal, interannual, as well as decadal timescales. Within the ''rectifier'' paradigm these timescales cannot be considered separately (i.e., by

low-pass filtering the model output to focus on the low-frequency component of variability).

[10] This paper is organized as follows. First, we present a description of the model configuration used for this study. As there is a paucity of data with which to validate the simulated biogeochemical fields over multiple decades, we begin with a comparison of the model control run with observations for the recent (data-rich) period. This allows for an evaluation of model biases. We then turn our attention to an analysis of three separate model experiments in order to describe the variability found on seasonal, interannual, and decadal timescales. We then present a consideration of the mechanisms responsible for the simulated variability. In the Discussion, we consider the relative strengths of the "regime shift" and "rectifier" frameworks for interpreting variability in the model.

2. Model Description

[11] The ocean model used here is ORCA2-LIM, which consists of the ORCA2 configuration of OPA version 8.2 [*Madec et al.*, 1998] coupled to the dynamic-thermodynamic Louvain-la-Neuve ice model (LIM) (see *Timmermann et al.* [2005], for a detailed description of the model). ORCA2 has approximately 2° horizontal resolution in the extra-tropics, with meridional resolution increasing to 0.5° at the equator. The ocean model includes 30 vertical levels, with 20 of these in the upper 500 m. The equation of state is calculated using the algorithm of *Jackett and McDougall* [1997]. Lateral mixing is oriented along isopycnal surfaces, and the parameterization of *Gent and McWilliams* [1990] for sub-grid-scale processes is used poleward of 10° latitude in either hemisphere. For vertical mixing, the turbulent kinetic energy (TKE) scheme of *Blanke and Delecluse* [1993] is used. No-slip boundary conditions are applied at solid lateral boundaries. This is the same configuration of the circulation model used in the previous studies of *Rodgers et al.* [2003] and *Rodgers et al.* [2004b], except that here we use the version of OPA which includes a free surface [*Roullet and Madec*, 2000]. The surface momentum forcing fields are taken from the daily mean wind stress fields from the NCEP reanalysis [*Kalnay et al.*, 1996] over the period 1948–2003. Surface heat fluxes are calculated using bulk formulas.

[12] Freshwater fluxes at the ocean surface (E-P) are calculated using the evaporative fluxes from the bulk formulas in conjunction with the precipitation fluxes from NCEP (1948–1978 and 2001–2003) and *Xie and Arkin* [1997] over 1979–2000. The free surface boundary condition is formulated such that ocean volume is globally conserved, as is the total salinity content of the ocean. Thus "nudging" of sea surface salinity is performed through a restoring flux of freshwater into the surface layer, with an equivalent timescale of relaxation of 12 d for the 10-m-thick surface layer to the monthly climatology of *Boyer et al.* [1998]. In this way, the salt content of the ocean is globally conserved. As the boundary condition for surface salinity will not in general be conservative with the corrective flux for freshwater, the net volume of water which is created or destroyed by this boundary condition at each time step is accumulated over the course of each year, and then a constant (spatially and temporally) corrective flux is applied at the sea surface over the following year to prevent the model volume from drifting.

[13] The biogeochemistry/food web model used here is the Pelagic Interaction Scheme for Carbon and Ecosystem Studies (PISCES) [*Aumont and Bopp*, 2006; *Aumont et al.*, 2008]. In addition to accounting for the biogeochemistry of carbon, the model also includes the main nutrients (Fe, SiO_2, NO_3, and PO_4) which are known to limit the growth of phytoplankton in the ocean. The 24 tracers carried by the model include two phytoplankton size classes (nano-phytoplankton and diatoms), two sizes of zooplankton (microzooplankton and mesozooplankton) and two sizes of sinking particles. A more complete description of the model can be found in the study of *Aumont and Bopp* [2006].

[14] The model includes various sources of nutrients external to the ocean. Dust deposition of both Fe and SiO_2 is done using the seasonal climatological fluxes of *Tegen and Fung* [1995]. The mass fraction for Fe is set to a constant of 3.5% and for SiO_2 of 7.5%. River input delivers NO_3, PO_4, SiO_2, Fe, Alk and DIC, with concentrations for DIC and Alk taken from *Ludwig et al.* [1996], and the concentrations of the other tracers calculated using constant Redfield ratios typical of rivers. In addition to these two sources, there is an additional source of Fe due to the flux of Fe from sediments to the ocean interior, either by diffusive fluxes across the sediment/water interface, or by resuspension due to bottom boundary currents [*Johnson et al.*, 1999; *de Baar and de Jong*, 2001; *Moore et al.*, 2004]. In PISCES, there is a simplistic parameterization of this source. Because of the coarse resolution of ORCA2, the model bathymetry is not able to correctly represent the critical spatial scales of the ocean bathymetry. An example is the continental shelves, which typically have a width scale of 10–30 km, which can be approximately an order of magnitude less than the horizontal resolution of the model.

[15] In order to take submodel grid-scale bathymetric variations into account in the Fe source function, the model grid structure has been compared with the high-resolution ETOPO5 [*NOAA*, 1988] data set. An algorithm was developed whereby for each and every horizontal grid cell, the corresponding region in the ETOPO5 data set is considered. For each vertical level in the model corresponding to a particular horizontal grid point, the corresponding ocean bottom area from ETOPO5 (in fractional units) is saved, with the end result being a three dimensional array containing an equivalent area for the bottom bathymetry of the ocean for the ETOPO5 data set. The flux is proportional to this fractional area, and is also prescribed to decrease with depth, with the maximum value of the flux having been chosen to optimize the agreement between the model simulation and the observations.

[16] Using the aforementioned spinup states for circulation and biogeochemistry, three simulations were conducted online with ORCA2-PISCES. The first is PISCES Control (PISCCTL), which was forced with NCEP-1 reanalysis fluxes [*Kalnay et al.*, 1996] for both wind stress and surface buoyancy over 1948–2003 (see *Raynaud et al.* [2006] for a

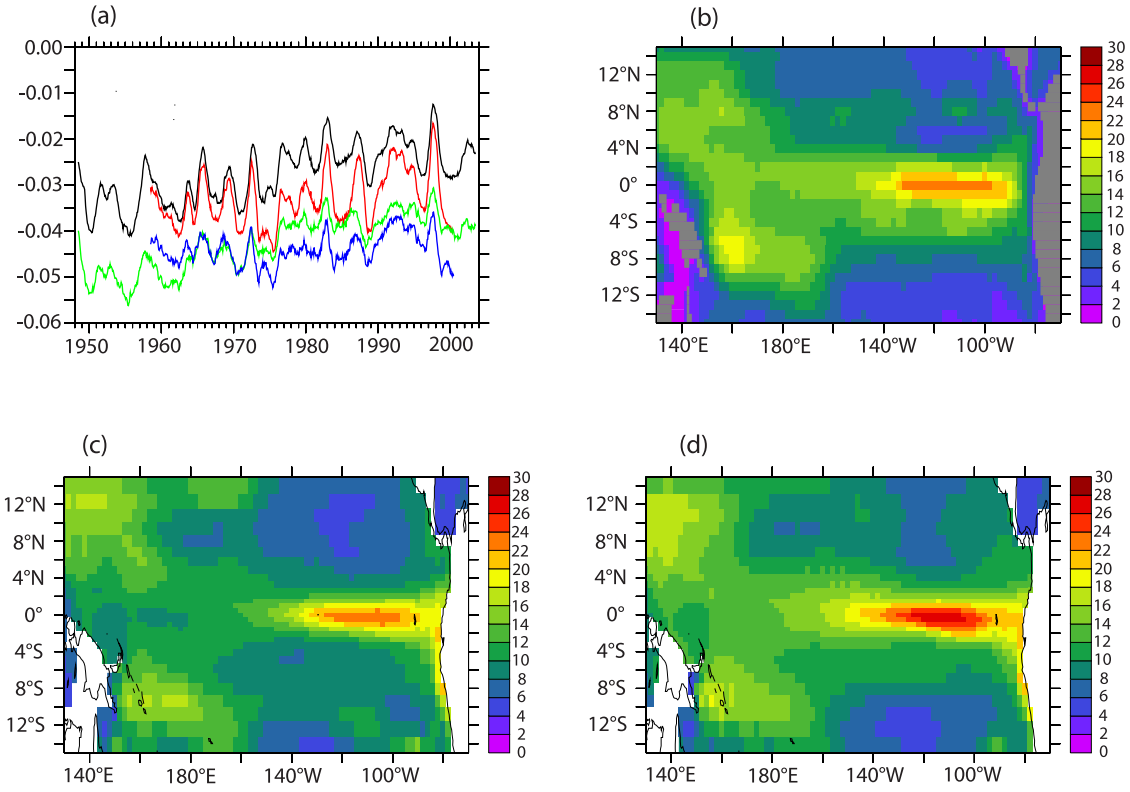

Figure 1. (a) Zonal wind stress averaged across equatorial Pacific waveguide (140°E-80°W, 2°N-2°S) for NCEP-1 (black) and ERA-40 (red) and averaged over 15°N-15°S for NCEP-1 (green) and ERA-40 (blue) (units: N/m^2). (b) Observations: root-mean-square (RMS) of linearly detrended monthly anomalies of the depth of the 20°C isotherm (Z20) over 1980–2000 (meters). (c) PISCCTL: RMS of linearly detrended monthly anomalies of Z20 over 1980–2000 (meters). (d) PISCERA: RMS of linearly detrended monthly anomalies of Z20 over 1980–2000 (meters).

description of this simulation, which they analyzed for North Atlantic air-sea CO_2 fluxes). The second simulation is CLIM_EQTAU (PISCES with climatologically varying equatorial wind stresses) which is otherwise identical to PISCCTL except that climatological wind stress forcing is used between 15°N-15°S in either hemisphere. For the CLIM_EQTAU experiment, a linear transition zone is used over the range 10°–20° latitude between the fully climatological values of wind stress at 10° latitude and the fully interannually varying wind stress at 20° latitude. Both the PISCCTL and CLIM_EQTAU experiments were designed and conducted within the framework of the European Northern Ocean Carbon Exchange Study (NOCES) project, a model intercomparison project for which NCEP-1 forcing was the protocol. After a preliminary analysis of the output from these simulations, it was decided to perform a third simulation using ERA-40 reanalysis [*Uppala et al.*, 2005] wind stresses at the sea surface over 1958–2001, while surface fluxes from NCEP-1 were used to calculate surface buoyancy fluxes. This third simulation is referred to as PISCERA. Thus the forcing fields for the three simulations differ only in their specification of the surface wind stresses.

[17] The PISCES biogeochemistry model was first spun up for 5000 years using monthly climatological ocean circulation fields until a set of convergence tests were satisfied. The state of the spunup PISCES model was then used as the initial condition for the simulations forced with interannually varying surface fluxes. The physical circulation model was initialized with *Boyer et al.* [1998] and *Antonov et al.* [1998] salinity and temperature climatologies and then spun up through two cycles of daily NCEP-1 reanalysis fluxes (over 1948–2003), for a total of 112 years. This period of 112 years was chosen as it is assumed that this is sufficient time for the upper wind-driven ocean circulation to adjust to first order.

[18] Unlike other tracers in the ocean, Fe is not strictly conserved in the PISCES model. For the original two simulations (PISCCTL and CLIM_EQTAU), Fe concentrations were maintained at a minimum of 0.01 nM. The justification for this was that the minimum values that have been measured in the real ocean are of order 0.02–0.03 nM (i.e., the measurement limit), so that setting a minimum value is a way of modeling unknown sources of Fe. However, a preliminary analysis of the output from the PISCCTL and CLIM_EQTAU simulations, it was decided to set a new lower limit for PISCERA at 0.005 nM, in order

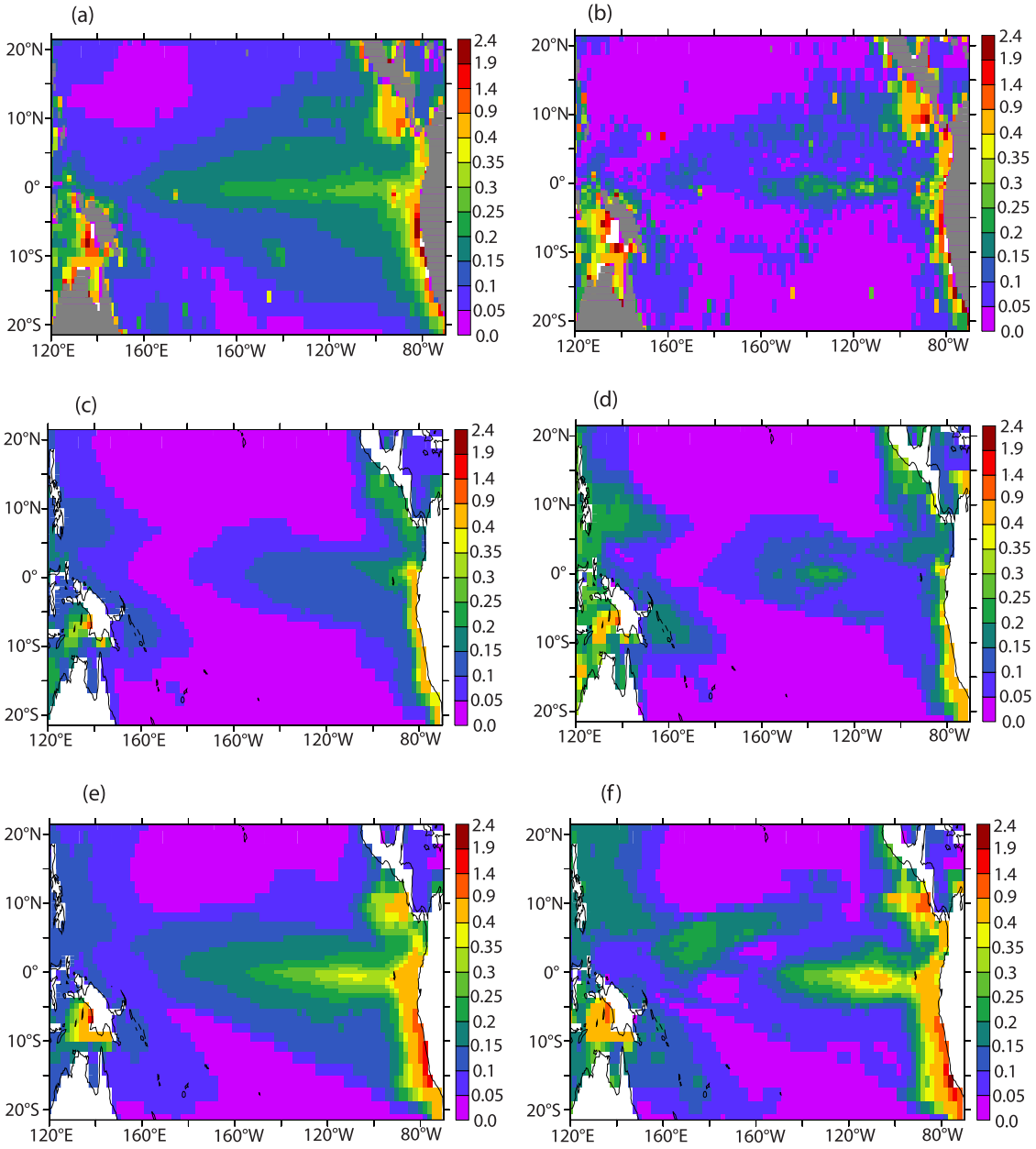

Figure 2. Chlorophyll concentration (mg/m^3). (a) SEAWIFS: mean over 1998–2002. (b) SEAWIFS: amplitude of climatological seasonal cycle over 1998–2002. (c) PISCCTL: mean over 1998–2002. (d) PISCCTL: amplitude of climatological seasonal cycle over 1998–2002. (e) PISCERA: mean over 1998–2001. (f) PISCERA: amplitude of climatological seasonal cycle over 1998–2001.

to test the extent to which the results are sensitive to this specification of a lower limit in Fe concentration.

3. Results

3.1. Comparison for Relatively Data-Rich Period

[19] As a prelude to an analysis of the model simulations, a comparison of time series of the zonal component of the surface wind stress over 4°N-4°S, 120°E-80°W (i.e., over the equatorial Pacific waveguide) is shown in Figure 1a for the NCEP-1 (black) and ERA-40 (red) reanalysis products. Analysis over this region is motivated by theoretical considerations from dynamical theory, according to which low-frequency changes in the slope of the thermocline across the equator is controlled by the integrated wind stress across the waveguide [*Cane and Sarachik*, 1981]. Additionally, the wind stresses averaged over a broader range (15°N-15°S, 120°E-80°W) are shown for NCEP (green) and ERA-40 (blue) in order to show how the equatorial changes relate to the large-scale changes in the trade winds. Large negative values indicate stronger trade winds.

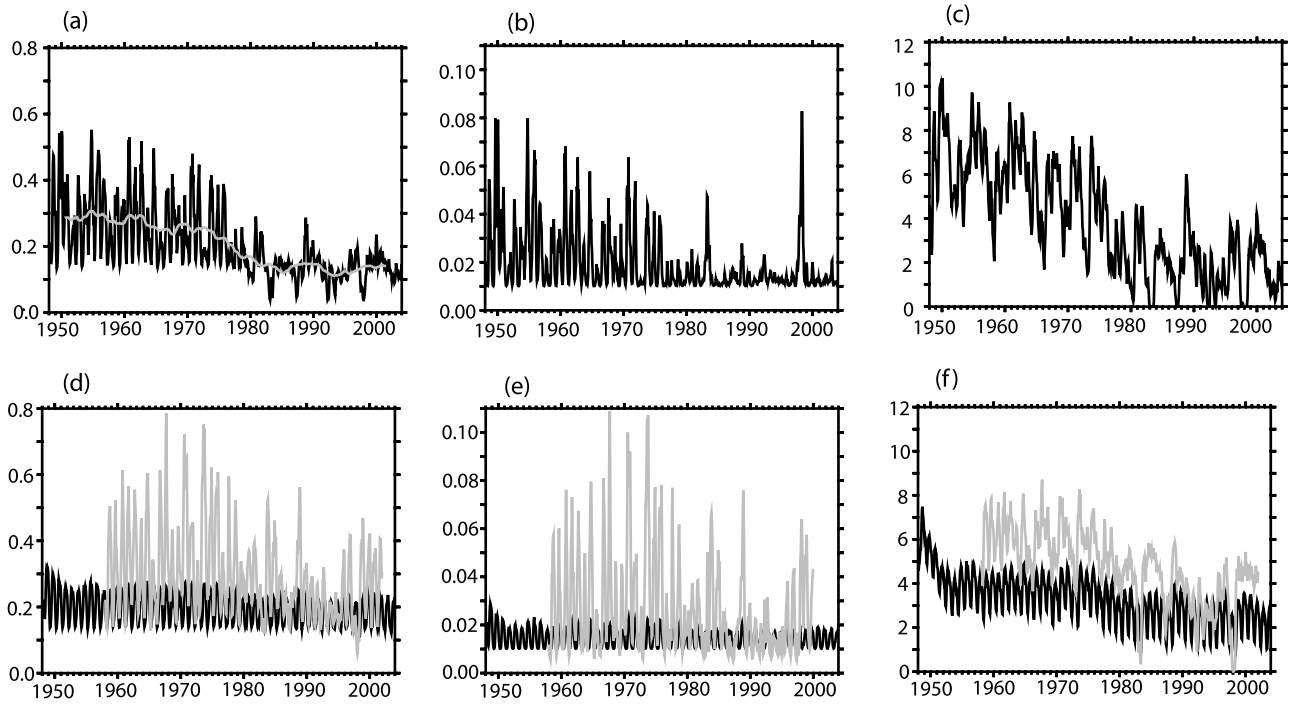

Figure 3. Time series of surface tracer concentrations averaged over 90–150°W, 2°N-2°S. (a) Chlorophyll for PISCCTL (mg/m^3) as monthly mean (black) and with 5-year running mean (gray). (b) Fe (nM) for PISCCTL. (c) NO_3 (μM) for PISCCTL. (d) Chl for CLIM_EQTAU (black) and PISCERA (gray). (e) Fe for CLIM_EQTAU (black) and PISCERA (gray). (f) NO_3 for CLIM_EQTAU (black) and PISCERA (gray).

This is an important diagnostic for decadal changes in mean conditions for the coupled ocean-atmosphere system in the equatorial Pacific that should be expected to have ramifications for ocean biogeochemistry and ecosystems. First, it is well known that for decadal variability of the coupled ocean/atmosphere system that the zonal slope of the equatorial pycnocline varies approximately linearly with this quantity. Second, on larger scales, it can be expected to be related to the overturning rate of the subtropical cells reported by *McPhaden and Zhang* [2002], i.e., to the rate of large-scale meridional overturning in the Pacific thermocline. Thus the fact that both reanalysis products exhibit a decrease in the absolute value of the integrated wind stress in 1976/1977 indicates that the zonal slope of the equatorial pycnocline will be reduced for the post-1976 period relative to the pre-1976 period. It can also be seen that the changes seen for the equatorial waveguide (4°N-4°S) are representative of the larger-scale changes for the tropical trade winds (15°N-15°S).

[20] Next we compare the root-mean-square (RMS) of the linearly detrended monthly anomalies of the depth of the 20°C isotherm (Z20) for the observations, the PISCCTL simulation, and the PISCERA simulation (the RMS for the CLIM_EQTAU simulation, which is not shown, is very small along the equator). Z20 is frequently used by physical oceanographers to characterize the depth of the pycnocline in the equatorial Pacific. The RMS from the data product of *Smith and Meyers* [1996] for the period 1980–2000 is shown in Figure 1b. The observations reveal a maximum along the equator in the eastern equatorial Pacific of amplitude 20 m. The equivalent field for PISCCTL (Figure 1c) indicates that this simulation is able to first order to capture the structure and amplitude of the variations along the equator. For the PISCERA experiment (Figure 1d) the model captures the correct structure of variability along the equator in the upwelling region, but the amplitude is somewhat overestimated.

[21] Next we compare the simulated surface Chl fields for the PISCCTL and PISCERA experiments with the observations from SEAWIFS. The mean surface Chl concentration from SEAWIFS over 1998–2002 (Figure 2a) is maximum along the coast of South America, with a tongue of locally maximum Chl extending along the equator from the coast of the Americas to the dateline. The amplitude of the seasonal cycle in the observations (Figure 2b) has been calculated by first constructing a monthly climatology over 1998–2002, and then for each horizontal surface grid point in this climatology calculating the difference between the seasonal maximum and seasonal minimum values. This reveals a maximum along the equator which between 100°W and 140°W is of nearly the same order as the mean concentration. In the central and eastern equatorial Pacific, there is also a secondary maximum between 5°N and 10°N, coinciding with the northern extension of the equatorial maximum in the mean (Figure 2a).

[22] The mean surface Chl concentration for the PISCCTL experiment (Figure 2c) exhibits a weak bias in its locally maximum concentration along the equator, and this weak bias is also found in the amplitude of the climatological seasonal cycle (Figure 2d) of the model output for the period 1998–2002. The locally maximum Chl concentration along the equator for PISCERA (Figure 2e) is in better agreement with the observations, as is the amplitude of the climatological seasonal cycle for the same experiment (Figure 2f). As the only difference between the PISCCTL and PISCERA experiments is in the wind stress forcing fields, and the ERA-40 equatorial wind stresses are thought to be more realistic than those in NCEP-1, this can help to explain the weak bias seen in the simulated Chl concentrations for NCEP.

3.2. NCEP Experiment: Surface Tracer Fields

[23] We begin our analysis of the PISCCTL experiment over the entire period 1948–2003 with a consideration of the surface tracer fields averaged over the upwelling region of the eastern equatorial Pacific (90–150°W, 2°N-2°S) in Figure 3. The time series of monthly surface Chl concentrations is shown in Figure 3a, and a 5-year running mean of the same field is superposed in gray. Figure 3a reveals a very large seasonality in surface Chl concentration in the upwelling region. Importantly, the surface Chl concentrations were significantly higher before 1976 than after 1976. Whereas seasonally minimum concentrations in this region do not change much during the experiment, it is the seasonally maximum concentrations (in July/August/September) that exhibit the largest modulations. The average Chl concentration for this region during the decade 1961–1970 (0.2624 mg/m^3) is 80% higher than the average concentration during the decade 1986–1995 (0.1429 mg/m^3). Referring back to the changes in the mean surface wind stress over the equatorial waveguide between these periods (Figure 1a), namely that the wind stresses are 34% higher for the earlier period, it is clear that there is an amplification in the response of Chl to these changes. It should be emphasized that this amplified response should not be viewed as a change in the background mean state for surface Chl concentrations, but rather as a modulation of the seasonally maximum concentrations. This underscores the importance of the seasonal cycle itself as an important component of understanding decadal changes. The behavior in the total Chl concentration is mirrored in both its diatom and nanophytoplankton components (not shown).

[24] Given that primary productivity in the equatorial upwelling region is Fe-limited, we turn our attention next to the monthly mean surface concentration of Fe averaged over the same region (90–150°W, 2°N-2°S) in Figure 3b. The figure reveals that there is a large decrease in Fe concentration between the pre-1976 and post-1976 periods in the equatorial upwelling region, with this change characterized by a significant modulation of the seasonally maximum values (July/August/September) with only minor changes in the seasonal minimum values. This time series confirms that decreased seasonality for Chl after 1976/1977 is reflecting decreased seasonality for Fe.

[25] The monthly surface NO_3 concentration averaged over the same region (90–150°W, 2°N-2°S) is shown in Figure 3e. For surface waters in the upwelling region, mean concentrations are 2.69 times larger for the decade 1961–1970 (5.50 μM) than for the later decade 1986–1995 (2.04 μM). In contrast to what was found for Chl and Fe, it is appropriate to refer to a decadal change in the mean state of NO_3, as there are large modulations of both the seasonal maximum and mean concentrations over the 56 years of the PISCCTL experiment. Thus for surface NO_3 the changes are better characterized as a change in the mean state, rather than simply being a modulation of the seasonal cycle.

[26] Next we consider the behavior of the CLIM_EQTAU and PISCERA experiments. In Figure 3d, the surface concentration of Chl is shown for the CLIM_EQTAU experiment (black) and PISCERA experiment (gray). For CLIM_EQTAU, the seasonal cycle in surface Chl tends to only experience minor modulations over the course of the 56 years of the experiment, in contrast to what was found with PISCCTL. Seasonally minimum values are in fact slightly higher for the 1970s than for the 1980s for CLIM_EQTAU, but these differences are an order of magnitude smaller than what was found for PISCCTL (Figure 3a). For PISCERA, as with PISCCTL, there are significant modulations of Chl concentrations on interannual to decadal timescales, with reduced amplitude of the seasonally maximum values after the late 1970s. The average Chl concentrations for the period 1961–1970 in the upwelling region (0.3411 mg/m^3) are 54.5% larger than the concentrations for the period 1985–1995 (0.2242 mg/m^3) with this difference in concentration being proportionally larger than the difference in wind stress between the two periods (17%).

[27] The surface concentration of Fe in the upwelling region is shown next in Figure 3e for the CLIM_EQTAU (black) and PISCERA (gray) experiments. For CLIM_EQTAU, there is a tendency for a regularly repeating seasonal cycle in Fe concentration, with only minor modulations of the amplitude of the seasonal cycle on interannual and decadal timescales. For PISCERA, on the other hand, the surface Fe concentration exhibits substantial modulation on interannual and decadal timescales, with decreased amplitudes after the mid-1970s. The equivalent time series for NO_3 concentrations is shown in Figure 3f.

[28] For CLIM_EQTAU there is in fact a shift toward decreased NO_3 concentrations that occurs approximately in 1980. Nevertheless this shift is significantly smaller than what was found for PISCCTL (Figure 3c). Figure 3f also reveals that for PISCERA there is a decrease in surface NO_3 concentrations, and that these changes are significantly larger than what is found for CLIM_EQTAU. Thus Figure 3 serves to demonstrate that for Chl, Fe, and (to a lesser extent) NO_3, that low-frequency changes in equatorial wind stress drive changes in surface ocean biogeochemical tracer concentrations that are proportionally significantly larger than the amplitude of the decadal changes in the wind stresses, and thereby the zonal slope of the equatorial thermocline. The consistency of the strongly amplified response with the PISCCTL and PISCERA experiments

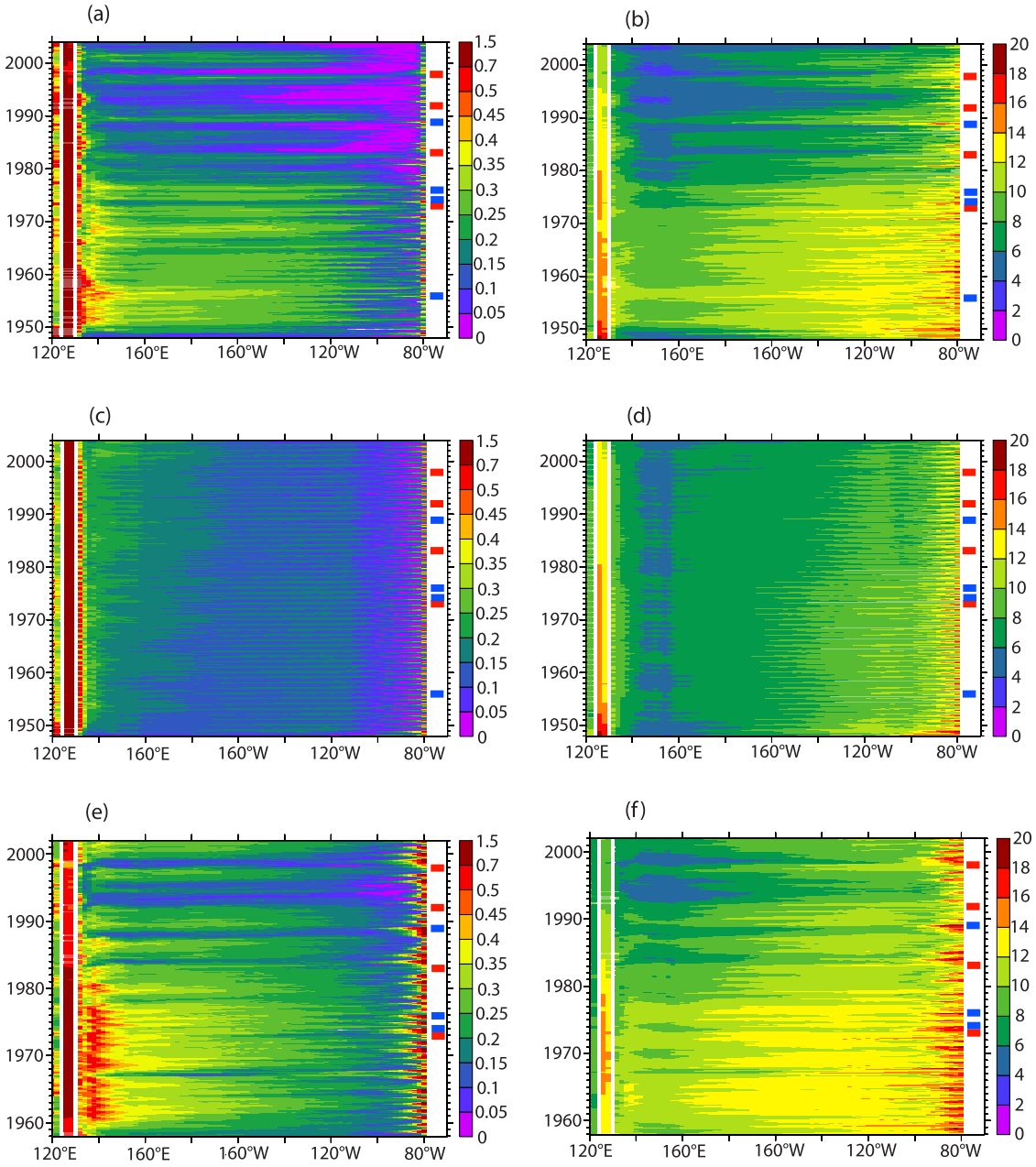

Figure 4. Tracer concentrations along 0°N projected onto σ_0 = 25.0 isopycnal surface; large El Niño (red bars) and La Niña (blue bars) events are shown immediately to the right of the color scale in each panel: (a) Fe for PISCCTL (nM); (b) NO_3 for PISCCTL (μM); (c) Fe for CLIM_EQTAU (nM); (d) NO_3 for CLIM_EQTAU (μM); (e) Fe for PISCERA (nM); (f) NO_3 for PISCERA (μM).

serves to underscore the robustness of the results obtained with the PISCCTL experiment.

3.3. Isopycnal and Circulation Diagnostics

[29] We have demonstrated that it is the equatorial wind stress component of the surface forcing (shown in Figure 1a) that is responsible for the decadal modulations of the seasonal cycle for PISCCTL and PISCERA (Figure 3). We now wish to turn our attention to an evaluation of the types of processes that could contribute to the large decadal changes seen in the PISCCTL and PISCERA experiments. In order to focus our analysis we consider three ways in which the supply of nutrients to the upwelling tongue of the eastern equatorial Pacific can change:

[30] 1. There are nonlocal processes which lead to decadal changes in tracer concentration on the isopycnal surfaces which feed the equatorial upwelling (i.e., within the EUC);

[31] 2. There are changes in the depth, or more precisely, the isopycnal horizon, from which upwelling water is drawn;

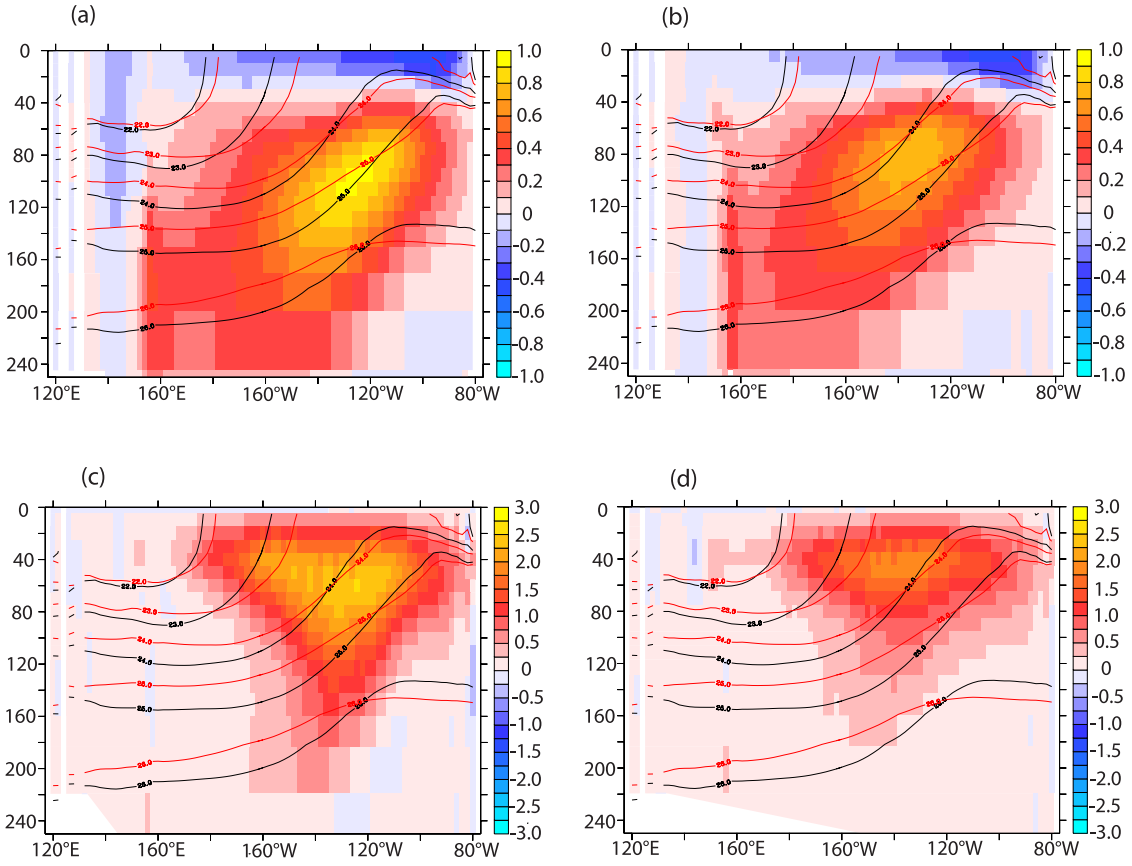

Figure 5. Model circulation diagnostics: For all panels, black contours indicate the mean potential density (referenced to the surface) averaged over 1961–1970, and red contours indicate the potential density averaged over 1986–1995. (a) Zonal velocity (m/s) along equator averaged over 1961–1970. (b) Zonal velocity (m/s) along equator averaged over 1986–1995. (c) Vertical velocity (m/d) along equator averaged over 1961–1970. (d) Vertical velocity (m/d) along equator averaged over 1986–1995.

[32] 3. There are local changes in the effective upwelling rate (volume/time).

[33] Clearly these three scenarios are by no means a priori mutually exclusive. In the analysis that follows, we will focus on the PISCCTL and CLIM_EQTAU experiments, as the results obtained with the PISCERA simulations are qualitatively very similar.

[34] First we consider changes in tracer concentration on isopycnal surfaces as they evolve along the equator with time, in order to address the first of the possibilities listed above. The evolution of Fe and NO_3 concentrations on the σ_0 = 25.0 isopycnal surface is presented in Figure 4 for the PISCCTL, CLIM_EQTAU, and PISCERA experiments. For each case, the strongest El Niño (red) and La Niña (blue) events over the last several decades are indicated as a series of bars immediately to the left of the color scale. The σ_0 = 25.0 isopycnal horizon corresponds approximately to maximum transport of the EUC, and thus changes in concentrations on this surface can be expected to impact the supply of nutrients to the upwelling region. The Fe concentration on this surface for PISCCTL (Figure 4a) reveals sizable variability on seasonal to decadal timescales. For interannual variability, concentrations tend to be low during warm El Niño events and high during cold La Niña events, with west-to-east advective propagation. These changes occur too rapidly to have propagated in from the extratropical source regions where this surface is ventilated (i.e. changes in preformed nutrients in the subducting regions) and suggest that processes under the warm pool may make a sizable contribution.

[35] Importantly, the model exhibits a large decrease in Fe concentration for the post-1976 period relative to the pre-1976 period. These changes are basin-scale, and the reduction in Fe concentration is proportionally larger than the 33% perturbation in the surface wind stress. Likewise, NO_3 on σ_0 = 25.0 exhibits a basin-scale decrease of concentrations during the late 1970s. The amplitude of this decadal shift is as large as the interannual variability on this surface. Unlike the situation with surface concentrations, there is a change in the mean state on this isopycnal surface. There is no suggestion after the 1997–1998 El Niño of a return to pre-1976 conditions, in contrast to what was reported for the thermocline circulation in the study of *McPhaden and Zhang* [2004].

[36] The corresponding Hovmoller diagrams for Fe and NO_3 along the equator on σ_0 = 25.0 for CLIM_EQTAU are

shown in Figures 4c and 4d, respectively. Here variability in concentration is largely limited to seasonal timescales. The absence of drift for CLIM_EQTAU indicates that the changes for the PISCCTL case (Figures 4a and 4b) are a response to low-frequency variability in the equatorial wind stress forcing for PISCCTL (Figure 1a), as the only difference between these experiments is that CLIM_EQTAU uses climatological wind stress forcing between 15°N and 15°S. Thus the decrease in tracer concentration on σ_0 = 25.0 for PISCCTL (Figures 4a and 4b) is associated with the decrease in the strength of the trade winds illustrated in Figure 1a.

[37] The equivalent Hovmoller diagrams for Fe and NO_3 for the PISCERA experiment are shown in Figures 4e and 4f. As with PISCCTL, for Fe there is a significant decrease in concentration after 1977, although there is a brief abrupt increase during 1979–1980 in the western Pacific which does not correspond to a La Niña event. The two periods in the 1990s corresponding to strong El Niño conditions show a significant decrease in Fe concentration, albeit with a delayed response in the east with respect to the surface temperature response. Likewise for NO_3, there is an abrupt decrease in concentration after 1976/1977, with the lowest concentrations occurring in the west associated with the two periods of strong El Niño conditions during the 1990s. For neither Fe nor NO_3 is there a clear signal of a return to pre-1976 conditions after the 1997/1998 El Niño.

[38] Having evaluated changes in tracer concentrations on isopycnal surfaces in the equatorial pycnocline, we now want to evaluate changes in circulation for the PISCCTL experiment (i.e., to consider the 2nd and 3rd scenarios listed above). The decadal changes in the zonal and vertical velocities considered as a function of longitude and depth along the equator are shown in Figure 5. For each panel, the velocity is shown in color shading, and black/red contours are overlain which represent the mean potential density fields for the decades 1961–1970 and 1986–1995 (the same contours are shown in each of the four panels), we see that for the σ_0 = 25.0 surface the mean pycnocline depth in the NINO3 region (90–150°W, 5°N-5°S) changed very little for the decadal "shift," but that this surface shoaled under the warm pool in the western equatorial Pacific.

[39] For the decade 1961–1970 (Figure 5a), the EUC core, as defined by maximum zonal velocity (in this case values of nearly 1.0 m/s) occurs at approximately 120–130°W, 80–110-m depth, and this corresponds approximately to the σ_0 = 25.0 surface. For the decade 1986–1995 (Figure 5b), the maximum zonal component of the velocity of the EUC is approximately 20% weaker, and occurs at a slightly lighter density horizon (σ_0 = ~24.5). This shoaling of the EUC core in density space between the decades of interest is roughly consistent with what was found in an earlier study [*Rodgers et al.*, 2004b].

[40] For the vertical velocity, it is clear that over the period 1961–1970 (Figure 5c) the σ_0 = 25.0 contour lies within the region where the mean upwelling rate exceeds 1.0 m/d for most of the longitudinal extent of the NINO3 box (90–150°W), whereas for the period 1986–1995 (Figure 5d) the σ_0 = 25.0 contour only overlaps the region where upwelling exceeds 1.0 m/d for a relatively small region near 100°W. This indicates that in addition to changes in the mean upwelling rate, the equatorial upwelling is drawing water from different ranges of isopycnal horizons for the different decades. Thus for each of the three scenarios listed earlier for how the supply of nutrients to the equatorial upwelling region can vary on decadal timescales, a reduction in the supply is expected for the 1986–1995 period relative to the 1961–1970 period.

[41] We have considered three separate scenarios by which there can be decadal changes in surface biogeochemical tracer concentrations in the upwelling region of the eastern equatorial Pacific, and found that all of them should contribute to a decrease in tracer concentration for the period 1986–1995 relative to 1961–1970. However, given that there is a significant amplitude effect on isopycnal surfaces (the first of the scenarios listed above), we are particularly interested in identifying the cause of these changes. The isopycnal analysis in Figure 4 indicated that the large changes in tracer concentration on the σ_0 = 25.0 surface are not local to the eastern equatorial Pacific, but rather span the entire basin. In order to identify the cause of these changes, we consider the mean Fe and NO_3 distributions along the equator as a function of depth for the respective decades.

[42] The time-mean distribution of Fe along the equator is shown for 1961–1970 in Figure 6a, for the decade 1986–1995 in Figure 6b, and the difference between these decades is shown in Figure 6e (1986–1995 minus 1961–1970). Fe concentrations are shown in color, and the mean density distribution for the decades 1961–1970 and 1986–1995 (black for the earlier decade, red for the later decade) is shown in contours. For each decade a surface maximum of Fe concentration can be seen in the upper 100 m (i.e., above σ_0 = 23.0) between New Guinea and 180°W, with concentrations reaching a minimum in density space between σ_0 = 23.0 and σ_0 = 24.0, with an increase in concentration for higher densities. The high surface concentrations are due to the fact that there is a large riverine input of Fe in this region, but also to the fact that primary productivity in this region is NO_3-limited (see *Gorgues et al.* [2007,

Figure 6. Fe(X,Z) concentration along equator as function of longitude and depth. For all panels, black contours indicate the mean potential density (referenced to the surface) averaged over 1961–1970, and red contours indicate the potential density averaged over 1986–1995. (a) Fe(X,Z) averaged over 1961–1970 for PISCCTL (nM). (b) Fe(X,Z) averaged over 1986–1995 for PISCCTL (nM). (c) Difference in Fe(X,Z) between decades 1961–1970 and 1986–1995 for PISCCTL (Figure 6b minus Figure 6a) (nM). (d) Difference in Fe(X,Z) between decades 1961–1970 and 1986–1995 for CLIM_EQTAU (nM). (e) NO_3(X,Z) averaged over 1961–1970 (μM). (f) NO_3(X,Z) averaged over 1986–1995 (μM). (g) Difference in NO_3(X,Z) between decades 1961–1970 and 1986–1995 for PISCINT (Figure 6e minus Figure 6d) (μM). (h) Difference in NO_3(X,Z) between decades 1961–1970 and 1986–1995 for CLIM_EQTAU (μM).

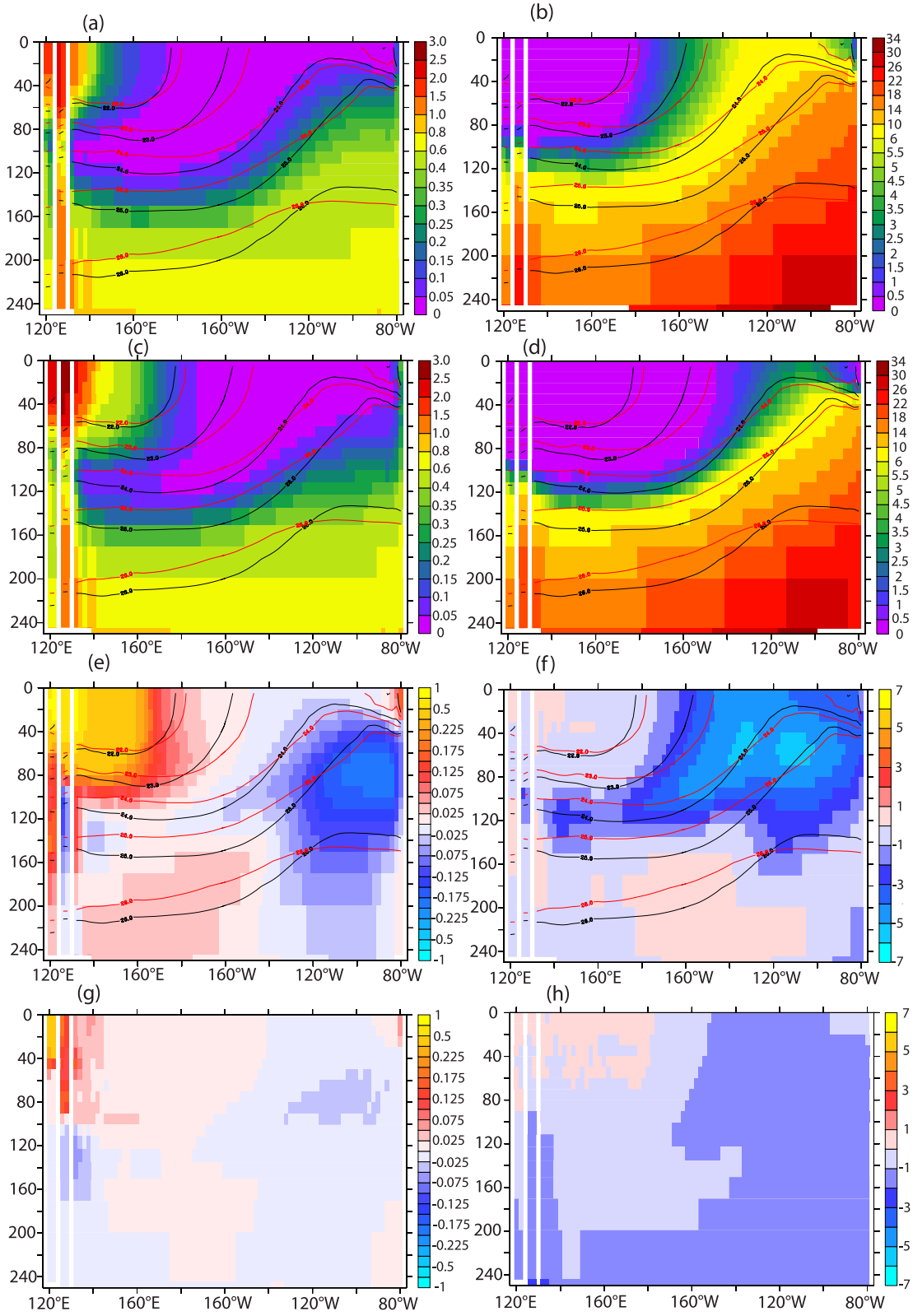
(a)
(b)
(c)
(d)
(e)
(f)
(g)
(h)
0
40
80
120
160
200
240
120°E
160°E
160°W
120°W
80°W
3.0
2.5
2.0
1.5
1.0
0.8
0.6
0.4
0.35
0.3
0.25
0.2
0.15
0.1
0.05
0
34
30
26
22
18
14
10
6
5.5
5
4.5
4
3.5
3
2.5
2
1.5
1
0.5
0
0.225
0.175
0.125
0.075
0.025
-0.025
-0.075
-0.125
-0.175
-0.225
-0.5
-1
7
5
3
1
-1
-3
-5
-7

Figure 6

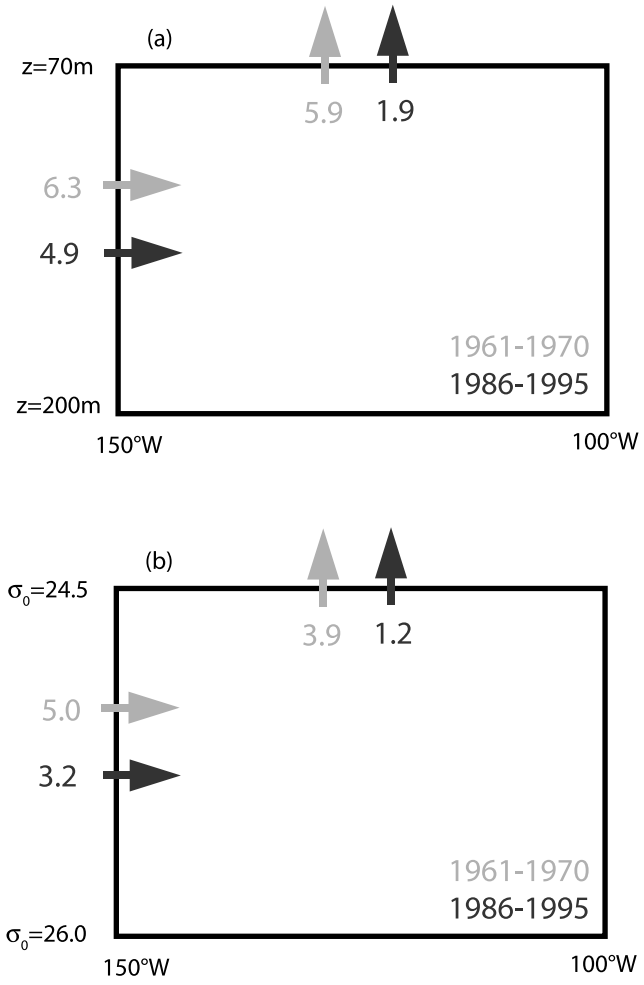

Figure 7. Schematic for advective Fe transport across boundaries of upwelling region (150–100°W, 5°N–5°S). (a) In-depth space, with lower boundary at 200 m and upper boundary at 70 m. (b) Viewed isopycnally.

Figure 3] and *Le Bouteiller et al.* [2003]). In the east, very low concentrations are found at the surface, but they increase monotonically with depth, with very large gradients in Fe concentration found over the isopycnal range σ_0 = 24.0 to 26.0.

[43] The change in Fe(X,Z) between these decades (i.e., 1986–1995 minus 1961–1970), shown in Figure 6c, reveals that for the pycnocline between 150°E and 180°E, the decadal changes in Fe concentration when considered as a function of depth are close to zero. Comparison with Figures 6a and 6b reveals that this is a region of sharp vertical gradients in the mean Fe distribution. Importantly, it can also be seen in Figure 6c that the mean depth of the σ_0 = 25.0 surface has changed by approximately 25 m between the two decades. The changes in the mean depth of this surface are significantly smaller averaged over the NINO3 region (90–150°W), indicating that the response of the thermocline slope to the decadal changes in surface wind stress are dominated by vertical displacements in thermocline depth under the warm pool. The changes in Fe concentrations for the same decades for CLIM_EQTAU are shown in Figure 6d, clearly demonstrating that the changes are significantly smaller there than with PISCCTL.

[44] The time-mean distribution of NO_3 as a function of longitude and depth along the equator is shown for the decade 1961–1970 in Figure 6e and for the decade 1986–1995 in Figure 6f (once again, the density for the respective decades is shown in color contours). It can be seen that NO_3 concentrations for the later period tend to be lower in the upper 150 m for the central and eastern equatorial Pacific, and this is revealed in the plot showing the difference between the decades (Figure 6g). The differences between the decades are quite small for water in the upper 100 m to the west of 180°W, but differences can also be seen in the upper region of the pycnocline, which corresponds to the lower reaches of the euphotic zone. This is in contrast to the case with Fe (Figure 6c), where differences between the decades are very small for this region of overlap between the pycnocline and the euphotic zone. The difference in NO_3 concentrations for the same decades for the CLIM_EQTAU simulation is shown in Figure 6h. Although smaller than the changes found for PISCCTL, the change does reproduce some of the structure of change found there.

[45] We have found for our control experiment (PISCCTL) that there are large decadal variations in surface Chl/Fe concentrations for the upwelling regions of the eastern equatorial Pacific. These are dominated by modulations of the amplitude of the seasonal cycle, with seasonally maximum concentrations having been significantly larger before the mid-1970s than after. An analysis of the model tracer fields on the σ_0 = 25.0 isopycnal surface led us to the interpretation that this shift in seasonal maximum surface concentrations is associated with the (nonlocal) shoaling of the pycnocline under the warm pool after 1976/1977, with this shoaling in the ocean model being a dynamical response to the weakening of the trade winds. According to this interpretation it is the abrupt relaxation of the equatorial wind stresses in 1976/1977 that causes the large modulation of the seasonal cycle in the tracer fields in the upwelling region in the model. Interestingly, we could not find a similar signal for the 1997/1998 transition described for the observed ecosystems by *Chavez et al.* [2003] or for the physical circulation by *McPhaden and Zhang* [2004].

[46] Thus far we have emphasized processes in the western equatorial Pacific pycnocline and how then can impact the supply of Fe to the upwelling region. However, this should not be taken to imply that local processes in the eastern equatorial Pacific do not also contribute to modulating the upwelling flux of Fe. Figure 7a shows schematically the transport of Fe into and out of a box bounded by 150–100°W, 70–200 m (with meridional boundaries at 5°N and 5°S). The horizontal arrows across the western boundary indicate the zonal advective flux of Fe (moles/s) for 1961–1970 (gray) and 1986–1995 (black) across 150°W from 5°N to 5°S. The vertical arrows denote the vertical advective flux across 70 m over 150–100°W and 5°N-5°S for 1961–1970 (gray) and 1986–1995 (black). Although

the zonal flux of Fe across 150°W is larger for the earlier than the later period, it can be seen that this only accounts for part of the change in the vertical supply upward across 70 m, thus implicating local changes in the eastern equatorial Pacific as contributing to the amplification.

[47] The changes in the advective fluxes are better considered within an isopycnal framework in Figure 7b. The upper and lower bounds of potential density chosen here (σ_0 = 24.5 and σ_0 = 26.0, respectively) bracket the EUC, while the lateral boundaries (150–100°W and 5°N-5°S) are the same as in Figure 7a. Viewed isopycnally, the change in the zonal flux across 150°W between the decades of interest is proportionally significantly larger than it is in depth space, with this difference due to nonlocal processes clearly making a first-order contribution to the changes in the upwelling flux between the decades 1961–1970 and 1986–1995.

4. Discussion

[48] As stated in the Introduction, we set out in this study to test the hypothesis that decadal changes in equatorial biogeochemistry and ecosystems are to first order controlled by variations in equatorial wind stress forcing. The simulations presented here have confirmed this hypothesis for the ORCA2-PISCES model configuration. The CLIM_EQTAU experiment reveals that Fe concentrations in the upwelling regions of the eastern equatorial Pacific only respond weakly to variability in the extraequatorial (poleward of 15° in either hemisphere) forcing, or to variability in equatorial buoyancy forcing. This result is consistent with ocean model experiments which have tested the extent to which intergyre exchange of extratropical temperature anomalies can impact temperatures in the equatorial Pacific pycnocline, i.e., models which have tested the mechanism for tropical Pacific decadal variability in physical state variables of the climate system proposed by *Gu and Philander* [1997] (see the studies of *Hazeleger et al.* [2001] and *Schneider et al.* [1999] for presentations of modeling results which demonstrate that the advective mechanism of *Gu and Philander* [1997] does not work for temperature anomalies). This by no means rules out the possibility that on longer timescales changes in the extratropics can cause a significant change in equatorial biogeochemistry. The CLIM_EQTAU experiment clearly demonstrates that it is local wind stress variability that controls the equatorial ecosystem response found in the PISCCTL experiment.

[49] Not only are decadal variability in equatorial biogeochemistry and ecosystems largely controlled by equatorial wind stresses, but their response is amplified relative to the decadal variations in surface wind stress forcing. We have seen in the control (PISCCTL) experiment that the decadal changes in surface Chl concentration in the upwelling region (80% larger for the period 1961–1970 than the period 1986–1995) are significantly larger than the associated changes in the depth of the pycnocline under the warm pool (or order ~20 m, or 30%), and significantly larger than the change in STC overturning strength reported by *McPhaden and Zhang* [2002]. The amplified response needs to be understood in its relation to the mean state. Throughout the experiment the vertical distribution of Fe along the equator under the warm pool is relatively stationary in depth space (Figure 6c). Because of the vertical proximity of the mean position of the pycnocline under the warm pool to the region where the mean vertical gradient of Fe concentration is greatest, relatively small changes in pycnocline depth can be manifested in proportionally larger changes in the concentration of Fe on isopycnal surfaces within the EUC. Given that the EUC is the dominant source of upwelling waters for the eastern equatorial Pacific, low-frequency perturbations to the mean depth of the pycnocline under the warm pool are reflected in changes in the advective supply of Fe to the euphotic zone along the equator in the eastern equatorial Pacific in July/August/September. In this way, the pycnocline and the ferrocline can become decoupled for decadal variability in the equatorial Pacific Ocean.

[50] The results form the PISCERA simulation attest to the robustness of the results found with PISCCTL. First, for PISCERA the biogeochemistry and ecosystem response in the upwelling region has an amplified response to the decadal changes in the wind stresses. Thus the results found with PISCCTL do not depend on the reanalysis fields used to force the model. Second, as was mentioned in the Introduction, the constraint for the minimum allowed Fe concentration in PISCCTL (0.01 nM) was relaxed for PISCERA (to 0.05 nM) as a means of testing the response of the model in regions where Fe concentrations are low. For PISCERA, the average Fe concentration in the upwelling region (gray curve in Figure 3e) gives seasonal minimum values that only rarely reach the imposed minimum concentrations. This is important, as it supports our interpretation that it is modulation of the Fe concentrations found during the upwelling season which are the main decadal response of Fe (and thereby Chl) in the upwelling region.

[51] To what extent are the "biological regime shift" and/or "rectifier" frameworks discussed in the Introduction appropriate for understanding the response of the equatorial Pacific ecosystems to decadal variability in the surface forcing? Whereas the surface wind stress forcing (Figure 1a) and the depth of the thermocline under the warm pool do exhibit decadal shifts, the response in surface Chl concentration in the upwelling region (Figures 3a and 3d) is better described by the decadal modulations of the amplitude of the seasonal cycle. These modulations reflect the fact that the changes in subsurface conditions are selectively transmitted to the surface during upwelling season. As such, the decadal change in the mean must be understood as a rectified response to changes in the seasonal cycle.

[52] We wish to emphasize that the results presented here do not rule out a role for extratropical variability in driving decadal changes in equatorial biogeochemistry. The surface NO_3 concentrations for CLIM_EQTAU (black curve in Figure 3f) exhibit a regime shift in their decrease in the late 1970s. What mechanism might be controlling this change? An examination of the NO_3 concentration on the σ_0 = 25.0 isopycnal (Figure 4d) demonstrates that this is not reflecting changes in NO_3 concentrations within the EUC.

One possibility is that the changes at the surface are being driven by variability in the winds over the Southern Ocean, which is able through planetary wave adjustment to very rapidly change the depth of the thermocline along the equator.

[53] Regarding the shift in the 1970s of the zonal component of wind stress within the equatorial waveguide (Figure 1a), there is continuing controversy over the extent to which this shift is realistic, or whether it is an artifact of the reanalysis product [*Wu and Xie*, 2003]. However, we wish to emphasize that the main result presented here is best understood as a process study, and does not rely upon the degree to which the shift in the NCEP wind stresses can be considered realistic. The extent to which biogeochemistry and ecosystems in the upwelling region exhibit an amplified response to low-frequency changes in the wind stress has potentially important implications for understanding how ecosystems may respond to global change. The study of *Vecchi et al.* [2006] argued that there has been a trend since the mid-19th century toward a shallower thermocline in the western equatorial Pacific, and if this trend were to continue into the 21st century (which would be consistent with the development of permanent El Niño conditions under global warming) one would expect further shoaling of the thermocline in the west. We leave as a subject for future investigation the question of the extent to which pycnocline/ferrocline decoupling will occur under greenhouse warming, and the extent to which these changes might serve to modulate the response of the biogeochemistry and ecosystems in the upwelling region to climate change.

[54] It is important to consider the extent to which the relatively strong amplification in the response of surface Chl in the model to low-frequency changes in wind stress is sensitive to the way in which the sediment sources of Fe to the ocean interior are prescribed in the model. In particular, the question arises to whether the stationarity in the vertical profile of Fe concentration (in depth space) under the warm pool is due to the large flux of Fe into the ocean interior in the western equatorial Pacific and the extent to which it is influenced or moderated by scavenging or remineralization effects. A more process-focused analysis of the role of the LLWBCs and their variability in maintaining Fe concentrations in the EUC is also left as a subject for future investigation.

[55] Here our intention was to focus on the response of ocean biogeochemistry and ecosystems in the upwelling region to time-varying forcing for the physical model. A complementary study (L. Ossiander, personal communication, 2008) considers the variations in equatorial biogeochemistry that result from time-varying sources of Fe for a climatologically varying ocean circulation, and in our future work we will consider the way both effects (variability in circulation and variability in Fe fluxes) impact greenhouse warming scenarios.

5. Conclusions

[56] Here we have presented a modeling study of biogeochemical and ecosystem variability for the upwelling regions of the eastern equatorial Pacific, with a coupled physical biogeochemical model. For the control run (PISCCTL), which was forced with NCEP-1 reanalysis fluxes, we have identified large changes in the surface Fe, Chl, and NO_3 concentrations in the upwelling region (90–150°W, 2°N-2°S) associated with the 1976/1977 "regime shift" in the equatorial Pacific. For Chl and Fe, surface concentrations are respectively 80% and 58% higher for the decade 1961–1970 than for the decade 1986–1995 with NCEP-1 forcing, and 92% and 55% higher with ERA-40 forcing. The changes in surface Chl and Fe are characterized by a large change in the amplitude of the seasonal cycle, and in particular it is found that there is a tendency for seasonally maximum concentrations in the upwelling region to be smaller after 1976 than before 1976. In this way, the change in equatorial ecosystems in 1976/1977 is best understood as a rectified response of the higher-frequency (seasonal) variability, rather than a regime shift or simply as a change in the mean state.

[57] An additional sensitivity study (CLIM_EQTAU) revealed that this shift in seasonality in the mid-1970s is to first order controlled by low-frequency variability in the equatorial wind stress forcing fields (between 15°N and 15°S), and that low-frequency variability in the extratropical forcing fields has only a small impact on the supply of Fe to the upwelling region on decadal timescales. Having identified that the forcing responsible for the equatorial ecosystem response lies in the equatorial region, we were motivated to conduct an additional experiment (PISCERA) forced with the ECMWF reanalysis fluxes in order to evaluate the robustness of results obtained with PISCCTL. The PISCERA simulation reproduced the amplified response in surface Fe, Chl, and NO_3 to low-frequency changes in the surface equatorial wind stress forcing. This sensitivity (amplification) should be understood as the main result of this study, as it has potentially important implications for climate change scenarios. For example, if under greenhouse warming the equatorial Pacific were to experience an El Niño–like perturbation in SST, with a corresponding decrease in the strength of the trade winds along the equator and a change in the thermocline structure, then this could have an impact on flux of Fe into the upwelling region by the EUC.

[58] Significantly, the presence of a time-invariant sediment source of Fe can substantially amplify the equatorial ecosystem response to changes in ocean circulation. The amplified response in equatorial Pacific ecosystems for both the PISCCTL and PISCERA simulations reflects a decoupling of the depth of the ferrocline and the depth of the pycnocline over the equatorial Pacific. This amplified response stands independently of the continuing controversy over the amplitude of the 1976/1977 shift as represented in the NCEP-1 reanalysis wind stresses for the equatorial Pacific [*Wu and Xie*, 2003]. The decoupling is due to the fact that while the ferrocline tends to have a stationary vertical distribution in the source regions of the EUC, the pycnocline depth can change as a response to change in the surface wind stress forcing. It is our hope that this work motivates further observational and modeling work to better understand the sources and sinks of Fe

in the ocean, as well as the time variability of Fe concentrations, as this could be very important for understanding the ecosystem response to climate change.

[59] **Acknowledgments.** We would like to thank Laurent Bopp, Jorge Sarmiento, Anand Gnanadesikan, Nicolas Metzl, Raghu Murtugudde, Gurvan Madec, Eric Galbraith, and the anonymous reviewer for their constructive comments. We would also like to thank Neville Smith for making his Z20 data product available to us. This report was prepared by Keith B. Rodgers under award NA17RJ2612 from the National Oceanic and Atmospheric Administration, U.S. Department of Commerce. The statements, findings, conclusions, and recommendations are those of the authors and do not necessarily reflect the views of the National Oceanic and Atmospheric Administration or the U.S. Department of Commerce. This work was also supported by the European Northern Ocean Atmosphere Carbon Exchange Study (NOCES) project (EVK2-CT2001-00134). The calculations were performed on the NEC SX-5 at Institut du développement et des ressources en informatique scientifique (IDRIS). This publication is partially funded by the Joint Institute for the Study of the Atmosphere and Ocean (JISAO) under NOAA cooperative agreement NA17RJ1232, contribution 1484.

References

Antonov, J., S. Levitus, T. P. Boyer, M. Conkright, T. O'Brien, and C. Stephens (1998), Temperature of the Pacific Ocean, *NOAA Atlas NESDIS 27*, vol. 2, 166 pp., U. S. Govt. Print. Off., Washington, D. C.

Aumont, O., and L. Bopp (2006), Globalizing results from ocean in situ iron fertilization studies, *Global Biogeochem. Cycles*, *20*, GB2017, doi:10.1029/2005GB002591.

Aumont, O., L. Bopp, and M. Schulz (2008), What does temporal variability in aeolian dust deposition contribute to sea-surface iron and chlorophyll distributions?, *Geophys. Res. Lett.*, *35*, L07607, doi:10.1029/2007GL031131.

Blanke, B., and P. Delecluse (1993), Variability of the tropical Atlantic ocean simulated by a general circulation model with two different mixed layer physics, *J. Phys. Oceanogr.*, *23*, 1363–1388, doi:10.1175/1520-0485(1993)023<1363:VOTTAO>2.0.CO;2.

Boyer, T. P., S. Levitus, J. Antonov, M. Conkright, O'T. Brien, and C. Stephens (1998), *World Ocean Atlas 1998*, vol. 5, *Salinity of the Pacific Ocean*, *NOAA Atlas NESDIS, 30,* 166 pp., U. S. Govt. Print. Off., Washington, D. C.

Cane, M. A., and E. S. Sarachik (1981), The response of a linear baroclinic equatorial ocean to periodic forcing, *J. Mar. Res.*, *39*(4), 651–693.

Chavez, F. P., J. Ryan, S. E. Lluch-Cota, and M. Ñiquen Carranza (2003), From anchovies to sardines and back: Multidecadal change in the Pacific Ocean, *Science*, *299*, 217–221, doi:10.1126/science.1075880.

Christian, J. R., M. A. Verschell, R. Murtugudde, A. J. Busalacchi, and C. R. McClain (2002a), Biogeochemical modeling of the tropical Pacific Ocean: II, Iron biogeochemistry, *Deep Sea Res., Part II*, *49*, 545–565.

Christian, J. R., M. A. Verschell, R. Murtugudde, A. J. Busalacchi, and C. R. McClain (2002b), Biogeochmical modeling of the tropical Pacific Ocean: I. Seasonal and interannual variability, *Deep Sea Res., Part II*, *49*, 509–543, doi:10.1016/S0967-0645 (01)00110-2.

Cibot, C., E. Maisonnave, L. Terray, and B. Dewitte (2005), Mechanisms of tropical Pacific interannual-to-decadal variability in the ARPEGE/ORCA global coupled model, *Clim. Dyn.*, *24*, 823–842, doi:10.1007/s00382-004-0513-y.

Coale, K. H., S. E. Fitzwater, R. M. Gordon, K. S. Johnson, and R. T. Barber (1996), Control of community growth and export production by upwelled iron in the equatorial Pacific Ocean, *Nature*, *379*, 621–624, doi:10.1038/379621a0.

de Baar, J. J. W., and J. T. M. de Jong (2001), Sources and sinks of iron in seawater, in *The Biogeochemistry of Iron in Seawater*, edited by D. Turner and K. Hunter, pp. 85–121, John Wiley, Hoboken, N. J.

Fine, R. A., R. Lukas, F. M. Binham, M. J. Warner, and R. H. Gammon (1994), The western Pacific: A water mass crossroads, *J. Geophys. Res.*, *99*, 25,063–25,080, doi:10.1029/94JC02277.

Gent, P. R., and J. C. McWilliams (1990), Isopycnal mixing in ocean circulation models, *J. Phys. Oceanogr.*, *20*, 150–156, doi:10.1175/1520-0485 [1990]020<0150:IMIOCM>2.0.CO;2.

Gorgues, T., C. Menkes, O. Aumont, J. Vialard, Y. Dandonneau, and L. Bopp (2005), Biogeochemical impact of tropical instability waves in the equatorial Pacific, *Geophys. Res. Lett.*, *32*, L24615, doi:10.1029/2005GL024110.

Gorgues, T., C. Menkes, O. Aumont, K. B. Rodgers, G. Madec, and Y. Dandonneau (2007), Indonesian throughflow control of the eastern equatorial Pacific biogeochemistry, *Geophys. Res. Lett.*, *34*, L05609, doi:10.1029/2006GL028210.

Gu, D., and S. Philander 1997, Interdecadal climate fluctuations that depend on exchanges between the tropics and extratropics, *Science*, *275*, 805–807, doi:10.1126/science.275.5301.805.

Hazeleger, W., M. Visbeck, M. A. Cane, A. R. Karspeck, and N. Naik (2001), Decadal upper ocean temperature variability in the tropical Pacific, *J. Geophys. Res.*, *106*, 8971–8988, doi:10.1029/2000JC000536.

Jackett, D. R., and T. J. McDougall 1997, A neutral density variable for the world's oceans, *J. Phys. Oceanogr.*, *27*, 237–263, doi:10.1175/1520-0485 [1997]027<0237:ANDVFT>2.0.CO;2.

Johnson, K. S., F. P. Chavez, and G. E. Friederich (1999), Continental-shelf sediment as a primary source of iron for coastal phytoplankton, *Nature*, *398*, 697–700, doi:10.1038/19511.

Kalnay, E. C., et al. (1996), The NCEP/NCAR reanalysis project, *Bull. Am. Meteorol. Soc.*, *77*, 437–471, doi:10.1175/1520-0477(1996)077<0437:TNYRP>2.0.CO;2.

Kawasaki, T. (1983), Why do some pelagic fishes have wide fluctuation in their numbers?: Biological basis of fluctuation from the viewpoint of evolutionary ecology, in *Reports of the Expert Consultation to Examine Changes in Abundance and Species Composition of Neritic Fish Resources*, edited by G. P. Sharp and J. Csirke, *FAO Fish. Rep.*, *291* ((2,3)), 1065–1080.

Kleeman, R., J. P. McCreary, and B. A. Klinger (1998), A mechanism for generating ENSO decadal variability, *Geophys. Res. Lett.*, *26*, 1743–1746, doi:10.1029/1999GL900352.

Latif, M., and T. B. Barnett (1994), Causes of decadal climate variability over the North Pacific and North America, *Science*, *266*, 634–637, doi:10.1126/science.266.5185.634.

Le Bouteiller, A., A. Leynaert, M. R. Landry, R. Le Borgne, J. Neveux, M. Rodier, J. Blanchot, and S. L. Brown (2003), Primary production, new production, and growth rate in the equatorial Pacific: Changes from mesotrophic to oligotrophic regime, *J. Geophys. Res.*, *108*(C12), 8141, doi:10.1029/2001JC000914.

Lehodey, P., F. Chai, and J. Hampton 2003, Modelling climate-related variability of tuna populations from a coupled ocean-biogeochemical-population dynamical model, *Fish. Oceanogr.*, *12*(4), 483–494, doi:10.1046/j.1365-2419.2003.00244.x.

Lluch-Belda, D., R. J. M. Crawford, T. Kawasaki, A. D. MacCall, R. H. Parrish, R. A. Schwartzlose, and P. E. Smith (1989), Worldwide fluctuations of sardine and anchovy stocks: the regime problem, *S. Afr. J. Mar. Sci.*, *8*, 195–2005.

Lluch-Belda, D., R. A. Schwartzlose, R. Serra, R. Parrish, T. Kawasaki, D. Hedgecock, and R. J. M. Crawford (1992), Sardine and anchovy regime fluctuations of abundance in four regions of the world oceans: A workshop report, *Fish. Oceanogr.*, *2*, 339–347, doi:10.1111/j.1365-2419.1992.tb00006.x.

Ludwig, W., J. L. Probst, and S. Kempe (1996), Predicting the oceanic input of organic carbon by continental erosion, *Global Biogeochem. Cycles*, *10*, 23–41, doi:10.1029/95GB02925.

Mackey, D. J., J. E. O'Sullivan, and R. J. Watson (2002), Iron in the western Pacific, a riverine or hydrothermal source for iron in the equatorial undercurrent?, *Deep Sea Res., Part I*, *49*, 877–893, doi:10.1016/S0967-0637(01)00075-9.

Madec, G., P. Delecluse, M. Imbard, and C. Levy (1998), OPA 8.1 general circulation model reference manual, in *Notes du Pole de Modelisation de l'Institut Pierre-Simon Laplace*, *11*, 91 pp. (available from http://www.lodyc.jussieu.fr/opa).

Mantua, N. J., S. R. Hare, Y. Zhang, J. M. Wallace, and R. C. Francis (1997), A Pacific decadal climate oscillation with impacts on salmon, *Bull. Am. Meteorol. Soc.*, *78*, 1069–1079, doi:10.1175/1520-0477 [1997]078<1069:APICOW>2.0.CO;2.

Martin, J. H., R. M. Gordon, and S. E. Fitzwater (1991), The case for iron, *Limnol. Oceanogr.*, *36*, 1793–1802.

Martin, J. H., et al. (1994), Testing the iron hypothesis in ecosystems of the Pacific Ocean, *Nature*, *371*, 123–129, doi:10.1038/371123a0.

McPhaden, M. J., and D. Zhang (2002), Slowdown of the meridional overturning circulation in the upper Pacific Ocean, *Nature*, *415*, 603–608, doi:10.1038/415603a.

McPhaden, M. J., and D. Zhang (2004), Pacific Ocean circulation rebounds, *Geophys. Res. Lett.*, *31*, L18301, doi:10.1029/2004GL020727.

Moore, J. K., S. C. Doney, and K. Lindsay (2004), Upper ocean ecosystem dynamics and iron cycling in a global three-dimensional model, *Global Biogeochem. Cycles*, *18*, GB4028, doi:10.1029/2004GB002220.

NOAA (1988), *Digital Relief of the Surface of the Earth*, *Data Announcement 88-MGG-02*, NOAA, Natl. Geophys. Data Cent., Boulder, Colo.

Raynaud, S., J. C. Orr, O. Aumont, K. B. Rodgers, and P. Yiou (2006), Interannual-to-decadal variability of North Atlantic air-sea CO2 fluxes, *Ocean Sci.*, *2*, 43–60.

Rodgers, K. B., B. Blanke, G. Madec, O. Aumont, P. Ciais, and J.-C. Dutay (2003), Extratropical sources of equatorial Pacific upwelling in an OGCM, *Geophys. Res. Lett.*, *30*(2), 1084, doi:10.1029/2002GL016003.

Rodgers, K. B., P. Friederichs, and M. Latif (2004a), Tropical Pacific decadal variability and its relation to decadal modulations of ENSO, *J. Clim.*, *17*, 3761–3774, doi:10.1175/1520-0442(2004)017<3761:TPDVAI>2.0.CO;2.

Rodgers, K. B., O. Aumont, G. Madec, C. Menkes, B. Blanke, P. Monfray, J. C. Orr, and D. P. Schrag (2004b), Radiocarbon as a thermocline proxy for the eastern equatorial Pacific, *Geophys. Res. Lett.*, *31*, L14314, doi:10.1029/2004GL019764.

Roullet, G., and G. Madec (2000), Salt conservation, free surface and varying volume: A new formulation for ocean general circulation models, *J. Geophys. Res.*, *105*, 23,927–23,942, doi:10.1029/2000JC900089.

Schneider, N., S. Venzke, A. J. Miller, D. W. Pierce, T. P. Barnett, C. Deser, and M. Latif (1999), Pacific thermocline bridge revisited, *Geophys. Res. Lett.*, *26*, 1329–1332, doi:10.1029/1999GL900222.

Schwartzlose, R. A., et al. (1999), Worldwide large-scale fluctuations of sardine and anchovy populations, *S. Afr. J. Mar. Sci.*, *21*, 289–347.

Smith, N. R., and G. Meyers (1996), An evaluation of expendable bathymermograph and Tropical Atmosphere-Ocean Array data for monitoring tropical ocean variability, *J. Geophys. Res.*, *101*, 28,489–28,510, doi:10.1029/96JC02595.

Tegen, I., and I. Fung (1995), Contribution to the atmospheric mineral aerosol load from land surface modification, *J. Geophys. Res.*, *100*, 18,707–18,726, doi:10.1029/95JD02051.

Timmermann, A. (2003), Decadal ENSO amplitude modulations: A nonlinear paradigm, *Global Planet. Change*, *37*, 135–156, doi:10.1016/S0921-8181(02)00194-7.

Timmermann, R., H. Goosse, G. Madec, T. Fichefet, C. Ethe, and V. Duliere (2005), On the representation of high latitude processes in the ORCA-LIM global coupled sea ice-ocean model, *Ocean Model.*, *8*, 175–201, doi:10.1016/j.ocemod.2003.12.009.

Uppala, S. M., et al. (2005), The ERA-40 re-analysis, *Q. J. R. Meteorol. Soc.*, *131*(612), 2961–3012, doi:10.1256/qj.04.176.

Vecchi, G. A., B. J. Soden, A. T. Witternberg, I. M. Held, A. Leetmaa, and M. J. Harrison (2006), Weakening of tropical Pacific atmospheric circulation due to anthropogenic forcing, *Science*, *441*, 73–76.

Wang, X., J. R. Christian, R. Murtugudde, and A. J. Busalacchi (2006), Spatial and temporal variability of the surface water pCO2 and air-sea CO2 flux in the equatorial Pacific during 1980–2003: A basin-scale carbon cycle model, *J. Geophys. Res.*, *111*, C07S04, doi:10.1029/2005JC002972.

Wu, R., and S.-P. Xie (2003), On equatorial Pacific surface wind changes around 1977: NCEP-NCAR reanalysis versus COADS observations, *J. Clim.*, *16*, 167–173, doi:10.1175/1520-0442(2003)016<0167:OEPSWC>2.

Xie, P., and P. A. Arkin (1997), Global precipitation: A 17-year monthly analysis based on gauge observations, satellite estimations, and numerical model inputs, *Bull. Am. Meteorol. Soc.*, *78*, 2539–2558, doi:10.1175/1520-0477(1997)078<2539:GPAYMA>2.0.CO;2.

O. Aumont, Centre IRD de Bretagne, 29280 Plouzané, France.

T. Gorgues, JISAO-School of Oceanography, Box 357940, University of Washington, Seattle, WA 98195-7940, USA.

C. E. Menkes, IRD, BP A5, 98848 Nouméa Cedex, New Caledonia.

K. B. Rodgers, Atmospheric and Ocean Sciences, Princeton University, Princeton, NJ 08544, USA. (krodgers@princeton.edu)